NASA/TM-20240000148 AIAA–2024–0520

Transient Optimization of an Electrified Gas Turbine Engine Using Machine Learning

Jonathan S. Litt, Jonathan L. Kratz, and Sonika Vuyyuru
Glenn Research Center, Cleveland, Ohio

Marcus A. Horning
HX5, LLC, Brook Park, Ohio

January 2024

NASA STI Program . . . in Profile

Since its founding, NASA has been dedicated to the advancement of aeronautics and space science. The NASA Scientific and Technical Information (STI) Program plays a key part in helping NASA maintain this important role.

The NASA STI Program operates under the auspices of the Agency Chief Information Officer. It collects, organizes, provides for archiving, and disseminates NASA's STI. The NASA STI Program provides access to the NASA Technical Report Server—Registered (NTRS Reg) and NASA Technical Report Server—Public (NTRS) thus providing one of the largest collections of aeronautical and space science STI in the world. Results are published in both non-NASA channels and by NASA in the NASA STI Report Series, which includes the following report types:

- TECHNICAL PUBLICATION. Reports of completed research or a major significant phase of research that present the results of NASA programs and include extensive data or theoretical analysis. Includes compilations of significant scientific and technical data and information deemed to be of continuing reference value. NASA counter-part of peer-reviewed formal professional papers, but has less stringent limitations on manuscript length and extent of graphic presentations.

- TECHNICAL MEMORANDUM. Scientific and technical findings that are preliminary or of specialized interest, e.g., "quick-release" reports, working papers, and bibliographies that contain minimal annotation. Does not contain extensive analysis.

- CONTRACTOR REPORT. Scientific and technical findings by NASA-sponsored contractors and grantees.

- CONFERENCE PUBLICATION. Collected papers from scientific and technical conferences, symposia, seminars, or other meetings sponsored or co-sponsored by NASA.

- SPECIAL PUBLICATION. Scientific, technical, or historical information from NASA programs, projects, and missions, often concerned with subjects having substantial public interest.

- TECHNICAL TRANSLATION. English-language translations of foreign scientific and technical material pertinent to NASA's mission.

For more information about the NASA STI program, see the following:

- Access the NASA STI program home page at http://www.sti.nasa.gov

- E-mail your question to help@sti.nasa.gov

- Fax your question to the NASA STI Information Desk at 757-864-6500

- Telephone the NASA STI Information Desk at 757-864-9658

- Write to:
NASA STI Program
Mail Stop 148
NASA Langley Research Center
Hampton, VA 23681-2199

NASA/TM-20240000148 AIAA–2024–0520

Transient Optimization of an Electrified Gas Turbine Engine Using Machine Learning

Jonathan S. Litt, Jonathan L. Kratz, and Sonika Vuyyuru
Glenn Research Center, Cleveland, Ohio

Marcus A. Horning
HX5, LLC, Brook Park, Ohio

Prepared for the
AIAA SciTech Forum
sponsored by the American Institute of Aeronautics and Astronautics
Orlando, Florida, January 8–12, 2024

National Aeronautics and
Space Administration

Glenn Research Center
Cleveland, Ohio 44135

January 2024

Acknowledgments

The Transformative Aeronautics Concepts Program/Transformational Tools and Technologies Project under the NASA Aeronautics Research Mission Directorate sponsored this work.

This work was sponsored by the
Transformative Aeronautics Concepts Program.

Level of Review: This material has been technically reviewed by technical management.

This report is available in electronic form at https://www.sti.nasa.gov/ and https://ntrs.nasa.gov/

Transient Optimization of an Electrified Gas Turbine Engine Using Machine Learning

Jonathan S. Litt, Jonathan L. Kratz, and Sonika Vuyyuru*
National Aeronautics and Space Administration
Glenn Research Center
Cleveland, Ohio 44135

Marcus A. Horning
HX5, LLC
Brook Park, Ohio 44142

Abstract

Gas turbine engines are designed with sufficient margin to prevent stall under normal operating conditions throughout their life. This compromise ensures that during rapid accelerations, compressor operation remains stable, but at the cost of efficiency and thrust responsiveness. The design margin encompasses multiple sources of uncertainty and systematic deviances from the operating line, the largest of which is the transient allowance. This set-aside accounts for the temporary incoordination of the engine spools during an acceleration while still enabling it to meet the certification requirement to accelerate from low to high power within a specified time, and without experiencing overtemperature, surge, stall, or other detrimental factors. Electrification of the powertrain provides the opportunity to address this reserve and truly optimize the design. The addition of electric machines inherent in hybrid propulsion concepts offers a means to interact with the engine shafts such that the necessary margin can be reduced, which can positively impact the engine design. By adjusting the amount of power extracted from or injected to the engine spools by the electric machines during transient operation, excursions from the operating line can be minimized. Past work using a dynamic engine model has shown that optimization of the fuel flow schedule during acceleration can reduce the required margin while still meeting the time requirement, and results are further improved when combined with power injection and extraction. The current work uses machine learning through a genetic algorithm to address the problem holistically by concurrently optimizing the electric machine power command and fuel flow acceleration schedule using an updated, higher fidelity version of the original engine model.

1.0 Introduction

The FAA requires testing to certify that traditional commercial turbofan engines can accelerate from idle to high power within a specified time, and additionally that the engine can accelerate without experiencing overtemperature, surge, stall, or other detrimental factors (Ref. 1). This means that the engine controller must be designed to achieve a minimum performance in terms of transient response, while protecting engine operability by ensuring safe transition during large throttle changes. In addition, the controller must be designed such that it will maintain these standards throughout the life of the engine, even though the engine is subject to normal wear and tear that makes it more susceptible to stall and overtemperature as it ages. This type of robust design essentially guarantees effective engine operation

*NASA Office of STEM Engagement Intern, University of California Berkeley undergraduate.

between overhauls under normal use. It is common practice to limit the acceleration of turbofan engines to a standard profile in multiengine aircraft, one that even the most deteriorated engine can achieve, in order to reduce the impact of mismatched engines and thereby minimize the potential for yaw on take-off (Ref. 2).

The High-Pressure Compressor (HPC) is designed such that the operating line is far enough from the stall line to ensure that it will never stall under normal operation; this distance, called the stall margin (SM), is defined in Figure 1. The required stall margin consists of a stack-up of several components, the largest of which is the transient allowance, i.e., the amount set aside for the temporary stall margin decrease due to transient operation. Reference 2 lists the contributors to the HPC stall margin worst case stack-up, i.e., the various factors that must be accounted for to ensure that the engine does not stall on acceleration; they are shown in Table I. The total of 24.4 percent indicates the distance the designed steady state working line must be from the stall line in order to ensure safe operation of a typical civil aero-engine HPC throughout the life of the engine under normal use. Some of the components of the stack-up are random, the remaining are systematic deviances related to deterioration or type of operation. Potentially, some of the latter group can be estimated. Algorithms such as weighted least squares and Kalman filters are used for these tasks (Refs. 3 and 4). This type of information enables the required stall margin reserve to be reduced because the portion required for each component of the stack-up that is estimated will usually be less than its corresponding worst case (three sigma) stall margin set-aside. This means that it is known with some confidence that the whole reserve is not required.

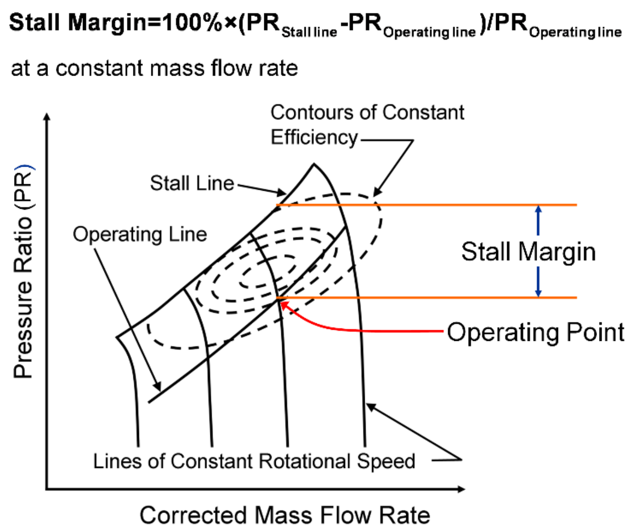

Figure 1.—Pressure Ratio (PR) of HPC vs. Mass Flow Rate, showing how Stall Margin (SM) is defined.

TABLE I.—EXAMPLE OF STALL MARGIN STACK-UP FOR THE HPC

Cause	Systematic deviances, percent	Random variances, percent
New production engine-to-engine working line variation	0	±1.5
New production engine-to-engine stall line variation	0	±4.0
In service working line deterioration	–2.0	-----
In service stall line deterioration	–4.0	-----
Control system fuel metering, and other actuators	0	±1.0
Reynolds number effects	–1.0	-----
Inlet distortion	–1.0	-----
Transient allowance	–12	-----
Total	–20	±4.4

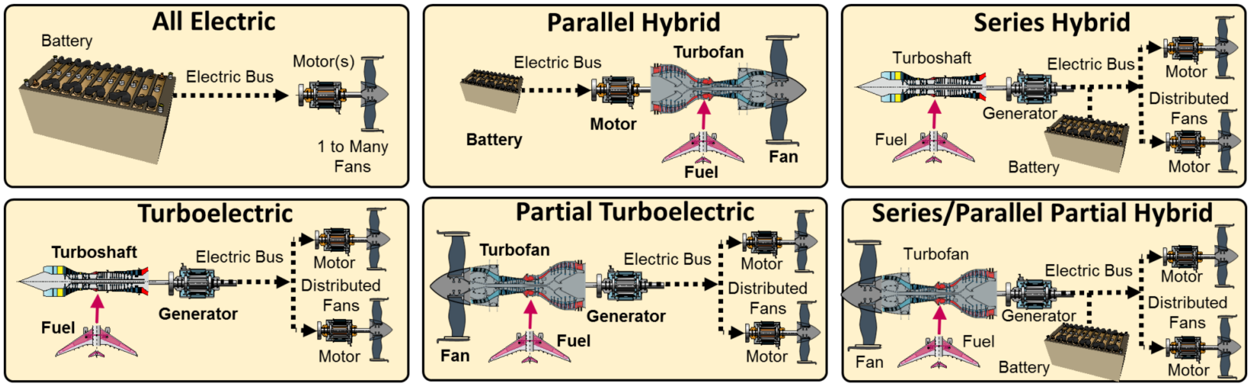

Figure 2.—Examples of electrified powertrain architectures.

Electrification of the aircraft powertrain provides fuel burn and emissions benefits when compared to the state-of-the-art, so there is a strong push in the industry to integrate electric machines (EMs) and thrust-producing fans with gas turbine engines (Figure 2). Of particular interest are the parallel hybrid and series/parallel partial hybrid architectures, which incorporate both a thrust-producing gas turbine engine and electrical energy storage. Nominally, EMs are connected to the engine shafts to generate power that is used to drive fans for producing thrust. However, the existence of the EMs enables dynamic interaction beyond that of a load. Taking advantage of the energy storage device to source or sink power, the fans can essentially be decoupled from the engine. By using the Turbine Electrified Energy Management (TEEM) Control algorithm to coordinate the loads on the shafts during an engine transient, the excursion toward stall can be greatly decreased (Refs. 5 and 6). This means that the potential exists to reduce the transient portion of the design stall margin.

The rest of this paper is organized as follows. Section 2.0 covers previous work using genetic algorithms to minimize transient excursions from the operating line. Section 3.0 describes how the engine model was updated for the present effort. Section 4.0 details the optimization approach used here while Section 5.0 presents results. These are followed by conclusions in Section 6.0.

2.0 Past Work

Previous work utilized genetic algorithms to develop fuel flow and power schedules that minimized the transient excursion from the operating line in an electrified gas turbine engine model. This section describes the engine model used in that previous work, which was subsequently updated as explained later, and the results of the prior work.

2.1 Engine Model

The testbed for the previous work was the NASA concept Advanced Geared Turbofan 30,000 (AGTF30) (Ref. 7). The AGTF30 is a model of a conceptual two-spool geared turbofan capable of producing ~30,000 lbf of thrust at sea level static (SLS) conditions. The AGTF30 is meant to represent technology that will be available in 2035; it includes features such as a compact gas turbine core and a variable area fan nozzle. The engine model is coded in the MATLAB/Simulink® environment using the NASA-developed Toolbox for Modeling and Analysis of Thermodynamic Systems (T-MATS) (Ref. 8). The model includes a realistic full-flight envelope controller (Ref. 9) that contains schedules for the variable area fan nozzle and variable bleed valve. It also has closed-loop gain-scheduled Proportional-Integral (PI) controllers for the fuel flow rate that include a nominal corrected fan speed controller and various limit controllers. Among the limit controllers are limiters for over-speed and over-temperature conditions. The model also includes acceleration and deceleration limit logic, implemented as a maximum Ratio Unit (RU) limit schedule for acceleration and a minimum RU limit schedule for deceleration. The RU schedules are defined as fuel flow divided by static pressure at the high-pressure compressor exit ($w_f/Ps3$). The various fuel flow rate commands go through a max-min decision tree to determine which command to use. Health parameters in the engine model set the health state of the turbomachinery components. Health parameters are modifiers that shift the flow capacity and efficiency of the compressors and turbines based on degradation. The engine model was subsequently updated to include an electrical power system to implement TEEM (Ref. 6).

2.2 Review of Prior Study

Previous work used genetic algorithms to optimize the fuel flow input profile during transients, from which an acceleration schedule was derived (Ref. 10). Subsequently, this optimized fuel flow input profile was leveraged in the optimization of TEEM control using electric machines interfaced with each engine shaft (Ref. 11). This work demonstrated how, using the electrified AGTF30 model, it is possible to collapse the transient response onto the operating line while still achieving an acceptable thrust response. It also demonstrated the tradeoffs between electric machine size, thrust responsiveness, and transient operability. It should be noted that originally TEEM was implemented as a closed-loop controller that attempted to maintain steady-state shaft speed versus fuel flow conditions during a transient (Refs. 5 and 6). While this approach demonstrated the utility of TEEM, it is not inherently optimal, and it requires the addition of logic for activation of the control. In References 10 and 11, an optimal solution was explicitly sought, subject to constraints placed on the fuel flow and power profiles, and the transient operability was shown to improve. The constraints on the input profiles were guided by understanding developed through observations from studies such as in References 5 and 6; furthermore, the constraints were justified to make the optimization problem more practicable.

The current work builds on these past efforts. Machine Learning (ML) is used to alter the fuel schedule and allows similar torque shape adjustments into the TEEM control as a way to further modify the response. Some key differences in the current study are the addition of physical effects and the simultaneous optimization of both fuel flow rate and electric machine power inputs.

3.0 Model Updates

The new engine model incorporates two major updates that impact the results: heat soak and tip clearance.

3.1 Heat Soak

Heat soak refers to heat transferring between the gas path and the engine’s metal parts. This phenomenon can have a noticeable effect on engine performance. During an idle-to-full-power transient, for instance, the engine components will heat up, absorbing typically 30 percent of the excess fuel energy. Heat soak is especially significant on hot restart and cold soaked starts, where, respectively, the heat transfer has the effect of adding fuel or reducing fuel flow (Ref. 2).

3.2 Tip Clearance

The second major addition is turbine tip clearance modeling. The performance of a gas turbine engine is sensitive to the distance between the tips of its high-pressure turbine (HPT) blades and the turbine shroud that seals the gas path. This gap is known as the tip clearance. Although the low-pressure turbine and the compressors are also susceptible to the inefficiencies brought on by excessive tip clearance, HPT tip clearance typically has the greatest impact on engine performance. Poor sealing of the turbine blade tips can lead to flow leakages that reduce work extraction. Blade tip vortices can result as well, leading to flow interactions that could reduce turbine efficiency and flow capacity, as well as increase noise. In general, reducing the HPT tip clearance will improve turbine efficiency thus reducing fuel burn, and because the turbine is able to extract more work from the flow, the turbine inlet temperature and exhaust gas temperature (EGT) are reduced. For a large commercial turbofan engine, a change of 10 mils of HPT tip clearance correlates to approximately a 1 percent difference in specific fuel consumption at cruise and a 10 °C (18 °R) difference in exhaust gas temperature at takeoff (Ref. 12). Increased turbine efficiency equates to lower fuel consumption, and turbine temperature reduction leads to slower degradation of the gas path parts and longer time on wing for the engine. The model incorporates a fairly standard implementation of an active thermal tip clearance control that uses bleed air to heat or cool the turbine case, causing it to expand or contract (Ref. 13).

Both heat soak and tip clearance modifications utilize a heat transfer extension to the original AGTF30 model (Ref. 14). This model extension allows the relevant physical parts of the engine to be modeled in a way that represents the relevant geometry of the engine and can interact with the appropriate gas path variables. This enables the modeling of not only the heat transfer, but also the resulting changes in clearance due to thermal expansion and contraction. Additionally, turbine blade growth due to centrifugal forces at high rotational speed, which further impacts tip clearance, is incorporated in the model (Figure 3) (Ref. 15).

To accommodate the modified dynamics of the engine model, the PI control gains were updated.

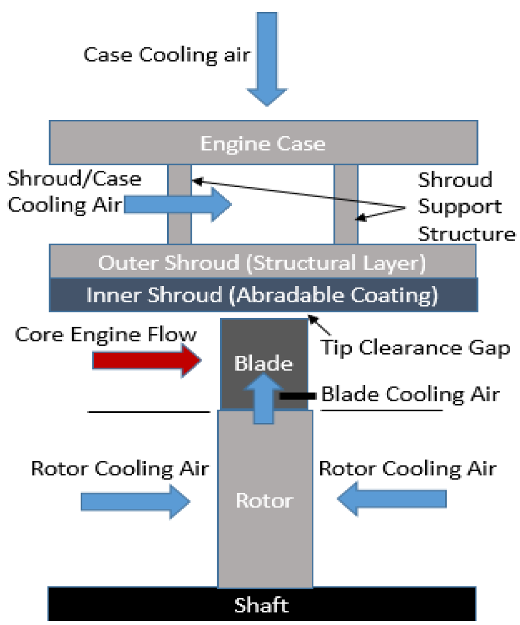

Figure 3.—Simplified schematic of the tip clearance model showing the structural pieces (rotor disk, blade, shroud/case) and the gas path temperature.

3.3 Accommodations for Updated Model

The new features added to the model clearly increase its sensitivity to temperature, including ambient temperature. This means that there is the potential for great performance variation between hot and cold day starts, which is certainly a realistic situation. For that reason, it is common practice at startup to hold the engine at idle to allow thermal soakage (Ref. 2). This brings the internal components to thermal equilibrium at a temperature higher than ambient, and therefore somewhat mitigates the effects of variation in ambient temperature. In the simulation, the metal temperatures are initialized to the values they would reach assuming sustained operation (at idle in this case) until thermal steady state is reached.

Furthermore, to simplify and keep the analysis more in line with certification practice, the testing here is performed on a new, undeteriorated engine at sea level static (SLS) standard day (59 °F) conditions (Ref. 16). The reference also mentions under 14 CFR § 33.89 - Operation Test, which incorporates the engine response requirements (14 CFR § 33.73 - Power or thrust response), that the certification test suite should include low temperature and high temperature tests (fluids and carcass) for starting and operating the engine. These tests are apparently meant to mimic ambient temperature variation, although as mentioned above, the prolonged idling at startup heats the internal components anyway before transient operation is attempted.

4.0 Optimization Approach

In addition to the model updates mentioned above, the other major difference from the previous work is that the fuel flow schedule and the torque input were optimized simultaneously rather than sequentially. As in the previous work, this effort utilized a genetic algorithm for optimization. This section describes the current approach, borrowing heavily from Reference 10 but updated to reflect the simultaneous optimization of the two inputs.

A genetic algorithm is a type of machine learning-based optimization scheme built upon the biological principles of natural selection and fitness (Ref. 17). Genetic algorithms tend to be less likely to converge to local minima or maxima than gradient based methods and are substantially more efficient than brute force methods. A population comprises numerous solution realizations, each with different parameters. Each individual solution is evaluated based upon a fitness function. The members of the population compete for survival into the next generation and for participation in reproduction. The genetic algorithm utilized in this study has the primary components of elitism, carry-over (replication), reproduction (crossover), and immigration. The primary sub-components of the genetic algorithm are selection, mutation, and duplicate removal. Each of these components and sub-components will be described in the following paragraphs. The sub-components are described first to set the foundation for describing the components.

The two selection methods used in this application were random and rank-based selection. In random selection, all members have the same probability of being chosen. In contrast, rank-based selection utilizes the pareto distribution (Ref. 18) and allows the user to specify parameters that define the exact shape. For instance, the 80 to 20 rule (Ref. 18) can be applied by specifying that the probability of selecting a member from the top 20 percent will be 80 percent.

Mutation creates a modified version of a member of the population. It will select the number of parameters to mutate based on specified probabilities and then will randomly select parameters to mutate. Finally, those parameters are mutated within specified bounds using a random distribution.

Duplicate removal applies whenever a duplicate shows up in the population. This feature will remove the duplicate and replace it with a new member that is generated within the specified parameter bounds using a random number generator.

Elitism involves advancing a set number of the most fit individuals to the next generation. Elitism seeks to preserve the best solutions and enables them to take part in finding better solutions through the functions of reproduction and mutation. In addition to advancing the elite, mutated variants of the elite may also be added to the next generation. This action promotes diversity but also exploits the high fitness of the elite. Inputs include the number of top members of the population to include in the elite, the number of the elite to mutate, the bounds for mutation, and the probability of mutating any number of parameters up to the full number of parameters.

The carry-over component of the algorithm selects members of the population, outside of the elite, to advance to the next generation. Mutation can apply as these members are carried to the next generation. The inputs include the number of members to carry over, the method of selection, inputs associated with the method of selection, and inputs associated with mutation including the bounds of mutation, the probability of a mutation occurring, and the probability of any number of parameters being mutated.

Reproduction consists of the combining of two members of the population to produce one or more new members of the population in the next generation. The offspring will derive its parameters from its parents. There are three methods for assigning parameters. The first is to inherit the parameter from one of the parents. The second is to average the parameters of the parents. The final is to randomly select a value for the parameter between the values of the parameter for the two parents. The probability of each method being used can be specified. In this application, each method had an equal chance of use. The parents are chosen based on the specified selection method, as is the number of offspring that a pair of members will produce. The combined fitness of the parents can be utilized to determine the number of offspring. Limits can be set for the number of times a single member of the population can participate in reproduction. In this application the number of offspring is specified. After the reproduction function is carried out, the offspring can be mutated given inputs about the probability of mutation, the bounds of mutation, and the probability of mutating any number of parameters.

Immigration refers to the introduction of new members to the population that will appear in the next generation. The new members are generated within the specified parameter bounds using a random number generator. This feature helps to explore the solution space more thoroughly.

In this application, the members of the population in the genetic algorithm define two parameters simultaneously: a RU limit schedule that defines the maximum ratio unit limit as a function of the corrected fan speed, and a power schedule profile for the transient. This is in contrast to previous works that separately optimized for populations of fuel flow commands and power schedules. The RU schedule was optimized rather than the fuel flow rate profile due to the incorporation of heat soak effects, which require additional fuel flow during the acceleration to make up for energy lost to the engine structure. The fuel flow rate profile continues to change beyond the fan speed transient, decreasing gradually as thermal equilibrium is achieved. The altered variation in the fuel flow rate response made it a bad candidate for optimization and thus the closed-loop fan speed set-point controller was leveraged, and the RU schedule was optimized directly. The RU limit schedule input profile is defined by nine points and correlates to the corrected fan speed. The end points of the schedule are fixed, and the interior points can be modified by the optimizer. The power schedule is defined by nine points between the maximum and minimum power level. The time at each data point in the profiles is fixed.

The variables in the optimizer associated with the RU schedule include seven values that define the maximum RU value at seven static corrected fan speeds between the minimum and maximum corrected fan speed values. Bounds are placed on the RU values to constrain the search space to reasonable solutions.

For the electric machines, the power input profile is defined by nine points between zero and the maximum power. To simplify the input profile and make the derivation of a practical schedule possible, the profile was constrained to start at full power at the beginning of the transient, remain there for some duration of the desired thrust response time, and then decrease monotonically until the power input returned to zero at the prescribed thrust response time. The variables in the optimizer include the fraction of the transient time spent at maximum power and the nine values between 0 and 1, *Y*, that are used to define the change in power between each of the nine data points that define the power profile as its magnitude decreases from its maximum value to zero. The time of each data point in this portion of the profile is spaced evenly. The EM power is a function of *Y*.

$$p_i = p_{i-1} - \frac{Y_i}{\sum_{j=1}^{9} Y_j} p_{max} \tag{1}$$

In Equation (1), *p* is the EM power, *i* is the index of the time interval that the EM power change occurs over, and the subscript "*max*" refers to maximum power capability of the EM, 750 hp in this case. For $i = 1$, the p_{i-1} term is equal to p_{max}. Note that this results in a time sequence, but it could be converted to a schedule that is a function of corrected fan speed error, as was done in Reference 11.

The optimizations consisted of simulations of the nonlinear AGTF30 model with different control inputs. The population was initialized using a random number generator to create 15 RU schedules and 15 power input profiles. The genetic algorithm was run for 10 generations. For each generation, the fitness of each combination of RU schedule and power input profile was evaluated (225 combinations in total in each generation). This entailed running a transient simulation and calculating the fitness for each member. The fitness, *f*, is defined in Equation (2) where *TSU* is the transient stack usage, i.e., the excursion from the operating line.

$$f = \frac{1}{TSU} \tag{2}$$

The thrust response time for an acceleration is the time to go from idle thrust to 95 percent thrust, which must not exceed 5 s. The *TSU* is a metric developed to quantify operability margin. The metric is a single value that quantifies the operability margin for a given transient. The metric is defined in Equation (3):

$$TSU = max\left(\frac{PR - PR_{SS}}{PR_{stall} - PR_{SS}}\right) \times 100\% \tag{3}$$

PR is the pressure ratio, PR_{SS} is the pressure ratio at the same corrected flow rate along the steady-state operating line, and PR_{stall} is the pressure ratio at the same corrected flow rate along the stall line (see Figure 1). Each of these variables represents a time sequence throughout the transient, so *TSU* equals the maximum value achieved by Equation (3) when evaluated at every time step. The *TSU* metric quantifies what portion of the compressor operability stack is used during the transient. By quantifying the operability margin with a single value for the entire transient using map data that considers the stall line and steady-state operating line, this metric summarizes the compressor operability without some of the nuances of stall margin. It is noteworthy that the fitness function could be modified to utilize other operability metrics, such as minimum stall margin, or combinations of various operability metrics.

The population was initialized using the optimal RU limit schedule profile and optimal power schedule profile from Reference 11 as one of the solutions. The "overall fitness" for each RU limit schedule member in the population was calculated to be the average fitness of that member across all power schedules. This means that the "overall fitness" for any given RU limit schedule member would be the sum of all fitness values of pairs that contain that RU limit schedule member, divided by the number of pairs that contain that RU limit schedule member. Similarly, the "overall fitness" for each power schedule member in the population was calculated to be the average fitness of that power schedule across all RU limit schedules. Then, the genetic algorithm used these "overall fitness" values as the fitness value for that member of the population to do any transformations, as it normally would.

5.0 Results

The optimization was carried out as described in the previous section. The genetic algorithm (GA) simultaneously identified an optimal RU schedule for accelerations and a power input profile for the high-pressure shaft (HPS) EM at SLS. The algorithm returned the same results for the final three generations, so it was considered to have converged. These results obtained with the updated model that includes heat soak and turbine tip clearance (TC) features are compared to the previous results (Ref. 11).

Figure 4 compares the maximum RU schedule that resulted from the GA optimization with and without heat soak and HPT TC effects. As can be seen, the two schedules are very similar. The schedule derived with heat soak and HPT TC effects is slightly more aggressive, particularly at low to moderate fan speeds. This could be due to the heat soak effects, which during the acceleration removes energy from the flow and demands additional fuel to accelerate the engine shaft to the desired setpoint in the same amount of time. Figure 5 shows the fuel flow rate and HPS EM power inputs. The new fuel flow rate is more aggressive on the acceleration and overshoots the final steady-state value. The overshoot is the result of heat soak as the engine must compensate for lost energy from the fluid into the engine structure through the combustion of additional fuel. The HPS EM power profiles are very similar. The primary reason for this is that the EM is saturated in both cases. If the EMs were unconstrained, more deviations could have been present.

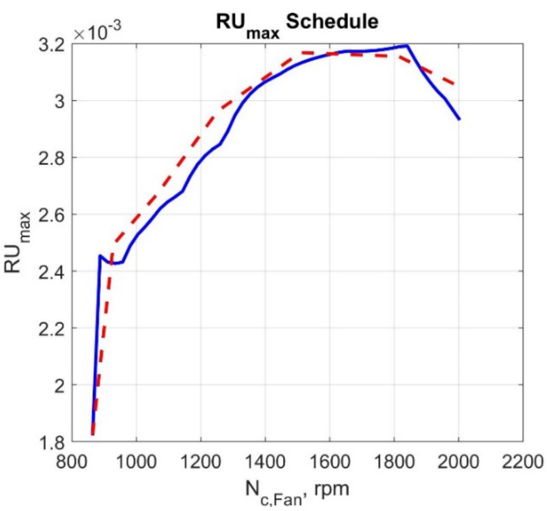

Figure 4.—RU acceleration schedule: original (solid blue), new (dashed red).

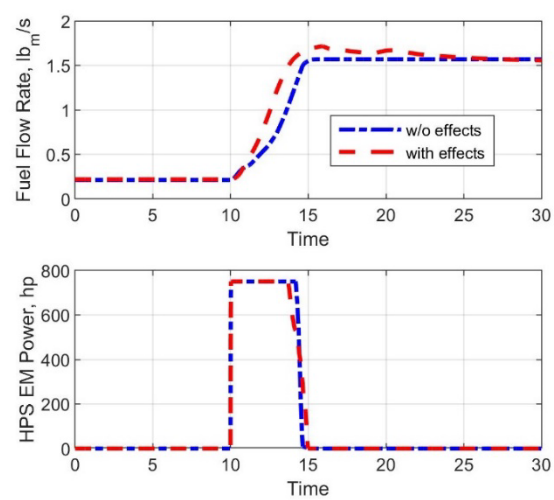

Figure 5.—Fuel flow rate and HPS EM power during a rapid acceleration.

Figure 6 shows the corrected fan speed, engine pressure ratio, and thrust responses. The new results have a more aggressive response with the same thrust response time as the results from Reference 11. It is hypothesized that the more aggressive response is related to the incorporation of heat soak and the need to increase fuel injection to accelerate the engine.

Figure 7 and Figure 8 show the temperatures and pressures at various locations in the engine. Here, the heat soak and TC effects are more directly observable. The heat soak impact is most evident in the temperature responses at the exit of the low-pressure compressor (LPC) (station 25), exit of the HPC (station 3) and most notably the exit of the low-pressure turbine (LPT) (station 5). Steady-state temperature discrepancies are also noted for stations 4 (HPT entrance), 45 (HPT exit), and 5 which are attributed to the HPT TC effects. This is primarily due to changes in HPT efficiency as a result of changes in HPT tip clearance. Similar results are reflected in Figure 8 with the pressures.

Figure 9 shows the HPC map with running lines for accelerations with and without the heat soak and TC effects. Also shown is the steady-state operating line in black, mostly covered by the transient running line without heat soak and TC effects. The deviation from the steady-state operating line with heat soak and HPT TC effects is more pronounced, but the results are still good. The additional movement toward the stall line is attributable to the more aggressive fuel flow input.

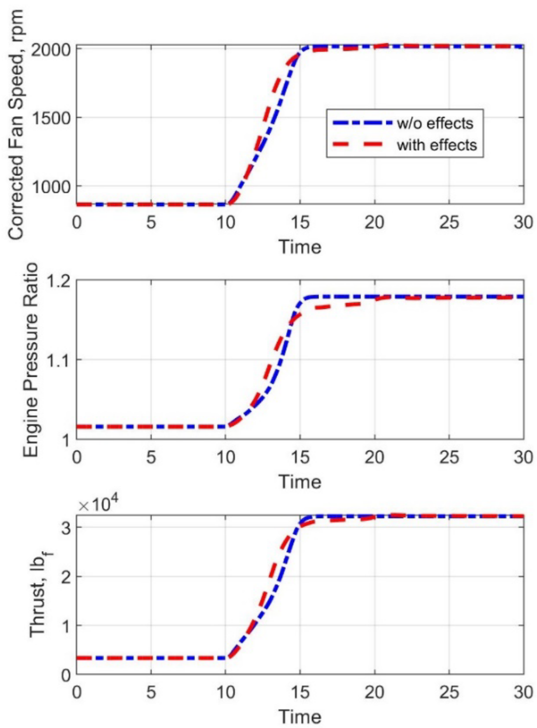

Figure 6.—Corrected fan speed, engine pressure ratio, and thrust responses.

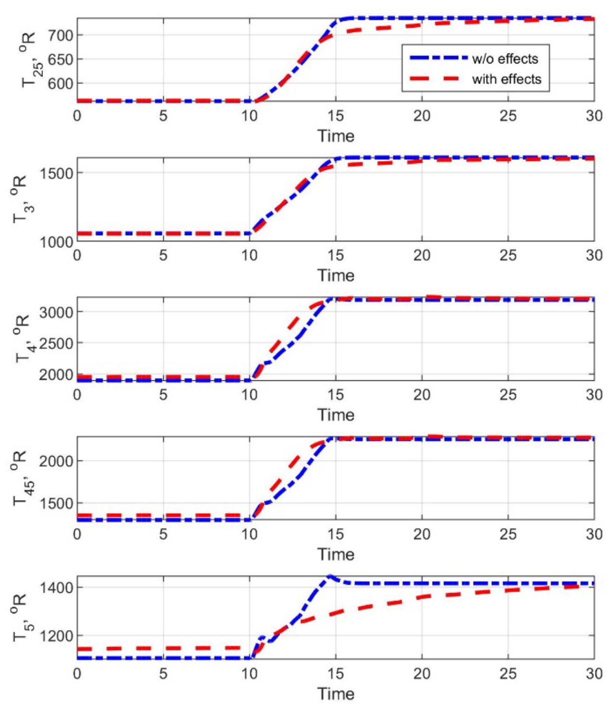

Figure 7.—Temperature responses at various stations within the engine.

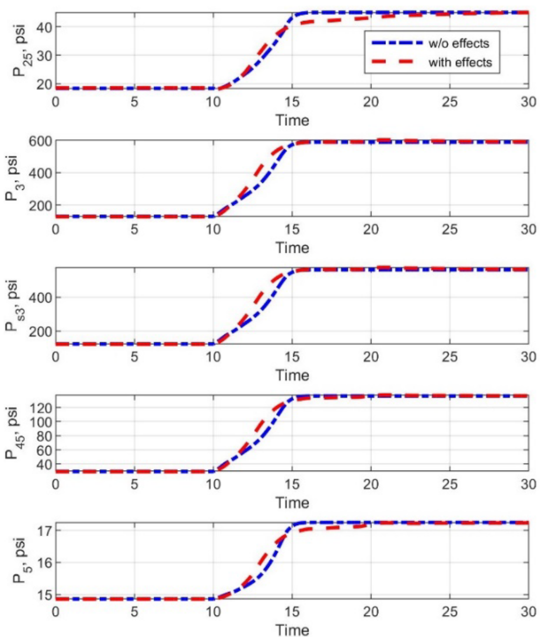

Figure 8.—Pressure responses at various stations within the engine.

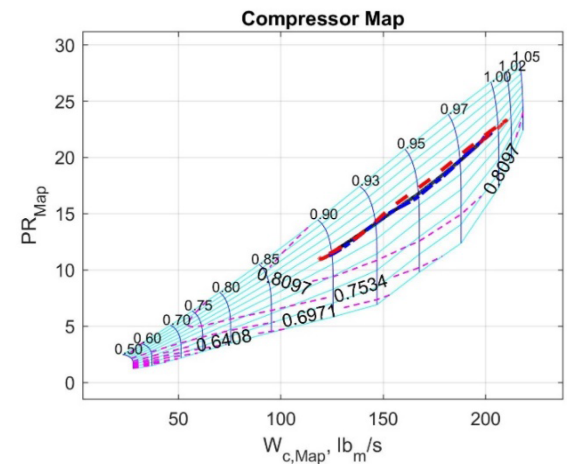

Figure 9.—HPC map showing original (solid blue), new (dashed red). The black dashed line is the steady state operating line.

6.0 Conclusions

The current work differed from past work in two ways: first, it used an updated model with heat soak and tip clearance effects, and second, it optimized the fuel flow and torque schedules simultaneously rather than sequentially. By making these two changes together, it makes it difficult to say which had the greater impact on the resulting schedules. However, when comparing the transient results for the two cases, it appears that the heat soak and tip clearance effects were significant, while the simultaneous optimization had less effect. The RU schedule generally demanded more fuel for a given pressure, which is expected when heat soak is taken into account because in the simulated scenario it removes energy from the flow. The power schedule was only slightly changed, and only at the end of the transient. The updated model’s transient response is quite different from those of the original model, although the rise time requirement is still met. While the new RU schedule is similar to the previous one, it appears to be slightly more aggressive, likely due to heat soak effects. Overall, the genetic algorithm performed successfully. The solution to which it converged was able to suppress the HPC transient excursion away from the operating line, although the deviation was larger than that for the original model, which did not incorporate heat soak. This is explained by the presence of the thermal transients and is probably more realistic, but that is not to say that a better solution does not exist. It is possible that the genetic algorithm would have found a better solution given more generations and a larger population size. Furthermore, the way the TEEM control optimization was constrained severely limited its ability to search for other solutions, although the power extraction limit was by far the most restrictive constraint on TEEM; having a larger EM would allow true torque shaping and thus could produce drastically different results, but a larger EM is also heavier. The ultimate goal of reducing the required transient component of the stall margin is that it could enable new, lighter engine designs without as much built-in margin. This highlights a major advantage of a data-driven solution that was not addressed here: estimation of other components of the stall margin stack. Machine learning’s ability to extract patterns from data could allow an algorithm to estimate an engine’s actual stall margin, accounting for the uncertainties that comprise the stall margin stack. This could be used not only to develop highly robust acceleration schedules, but also for stall avoidance as part of an advanced control scheme.

References

1. Federal Aviation Administration FAR Part 33—Airworthiness Standards: Aircraft Engines, Subpart E—Design and Construction; Turbine Aircraft Engines, Sec. 33.73, Power or thrust response.
2. Walsh, P.P., and Fletcher, P., *Gas Turbine Performance*, Blackwell Science/ASME, 2004.
3. D. Doel, “An Assessment of Weighted-Least-Squares-Based Gas Path Analysis,” *ASME Journal of Engineering for Gas Turbines and Power*, Vol. 116, April 1994, pp. 366–373.
4. Luppold, R.H., Roman, J.R., Gallops, G.W., and Kerr, L.J., “Estimating In-Flight Engine Performance Variations Using Kalman Filter Concepts,” AIAA-89-2584, AIAA 25th Joint Propulsion Conference, Monterey, CA, 1989.
5. Culley, D., Kratz, J., and Thomas, G., “Turbine Electrified Energy Management (TEEM) For Enabling More Efficient Engine Designs,” AIAA 2018-4798, *AIAA Joint Propulsion Conference*, Cincinnati, OH, 9–11 July 2018.
6. Kratz, J.L. Culley, D.E., and Thomas, G.L., “A Control Strategy for Turbine Electrified Energy Management,” AIAA Paper 2019–4499, *AIAA Propulsion and Energy Forum*, Indianapolis, IN, 19–22 August 2019.
7. Jones, S.M., Haller, W.J., Tong, M.T., “An N+3 Technology Level Reference Propulsion System,” NASA/TM—2017-219501, 2017.
8. Chapman, J., Lavelle, T., May, R., Litt, J., and Guo, T.-H., “Toolbox for the Modeling and Analysis of Thermodynamic Systems (T-MATS) User’s Guide,” NASA/TM—2014-216638, 2014.
9. Chapman, J.W., Litt, J.S., “Control Design for an Advanced Geared Turbofan Engine,” AIAA-2017-4820, Propulsion and Energy Forum, Atlanta, GA, June 10–12, 2017.
10. Kratz, J.L., “Transient Optimization of a Gas Turbine Engine,” AIAA 2023-0703, January 2023.
11. Kratz, J.L., Culley, D.E., Lehan, J., “Transient Optimization for the Betterment of Turbine Electrified Energy Management,” AIAA 2023-0704, January 2023.
12. Wiseman M.W., and Guo, T.-H., “An Investigation of Life Extending Control Techniques for Gas Turbine Engines,” Proceedings of the 2001 American Control Conference, Arlington, VA, 25-27 June 2001, pp. 3706–3707.
13. Lattime, S.B., and Steinetz, B.M., “Turbine Engine Clearance Control Systems: Current Practices and Future Directions,” NASA/TM–2002-211794, 2002.
14. Litt, J.S., “Harnessing the Digital Transformation for Development of Electrified Aircraft Propulsion Control Systems,” SAE Technical Paper 2023-01-1510, 2023.
15. Kratz, J., and Chapman, J., “Active Turbine Tip Clearance Control Research,” in *Sixth NASA Glenn Research Center Propulsion Control and Diagnostics (PCD) Workshop*, J.S. Litt, (Ed.), NASA/CP—2018-219891, April 2018.
16. Federal Aviation Administration, “Advisory Circular, FAR Guidance Material, Aircraft Engine Type Certification Handbook,” 33-2B, 1993 (cancelled 2013).
17. Brunton, S., and Kutz, N., Data-Driven Science and Engineering: Machine Learning, Dynamical Systems, and Control, Cambridge, United Kingdom, Cambridge University Press, 2019.
18. Newman, M., “Power Laws, Pareto Distributions and Zipf’s Law,” Contemporary Physics. 46 (5): pp. 323–351.